

UDC 620.186; 620.172

<https://doi.org/10.17073/0021-3438-2024-1-81-92>

Research article

Научная статья



Impact of ECAP at 300 °C on the microstructure and mechanical properties of the quenched Zr–2.5%Nb alloy

D.V. Gunderov^{1,2}, A.G. Stotskiy¹, S.D. Gunderova^{1,2}, V.R. Aubakirova¹, A.Yu. Demin¹¹ Ufa University of Science and Technology

32 Zaki Validi Str., Ufa, Republic of Bashkortostan 450076, Russia

² Institute of Molecule and Crystal Physics of the Ufa Federal Research Centre of the RAS

71 Oktyabrya Prosp., Ufa, Republic of Bashkortostan 450054, Russia

✉ Andrey G. Stotskiy (stockii_andrei@mail.ru)

Abstract: We investigated the microstructure of the Zr–2.5%Nb zirconium alloy after subjecting it to equal-channel angular pressing (ECAP) and found that ECAP at 300 °C increases the strength by 1.4–1.8 times. Notably, unlike other studies, our alloy did not show complete dissolution of niobium particles, which may be due to the reduced diffusion rates at the lower deformation temperature of 300 °C. Pre-treatment involving quenching before severe plastic deformation was also studied, which developed a lamellar structure introducing additional boundaries that facilitated grain refinement during subsequent ECAP. The strength of the alloy was further enhanced by solid-solution hardening, achieved through the complete dissolution of the Nb particles into the matrix post-quenching. This process resulted in a 2.3-fold increase in yield strength after quenching plus ECAP compared to the initial coarse-grained state.

Keywords: microstructure, quenching, equal channel angular pressing, strength, Nb particles, Zr–2.5%Nb zirconium alloy.

Acknowledgments: This work was carried out with financial support from the Russian Science Foundation under Project № 20-79-10189-П, <https://rscf.ru/en/project/23-79-50039/>

Mechanical tests and microstructure study were carried out in the Center for collective use «Nanotech» of Ufa University of Science and Technology.

For citation: Gunderov D.V., Stotskiy A.G., Gunderova S.D., Aubakirova V.R., Demin A.Yu. Impact of ECAP at 300 °C on the microstructure and mechanical properties of the quenched Zr-2.5%Nb alloy. *Izvestiya. Non-Ferrous Metallurgy*. 2024;30(1):81–92.

<https://doi.org/10.17073/0021-3438-2024-1-81-92>

Влияние РКУП при температуре 300 °С на структуру и свойства закаленного сплава Zr–2,5%Nb

Д.В. Гундеров^{1,2}, А.Г. Стоцкий¹, С.Д. Гундерова^{1,2}, В.Р. Аубакирова¹, А.Ю. Демин¹¹ Уфимский университет науки и технологий

Россия, 450076, Респ. Башкортостан, г. Уфа, ул. Заки Валиди, 32

² Институт физики молекул и кристаллов Уфимского федерального исследовательского центра РАН

Россия, 450054, Респ. Башкортостан, г. Уфа, пр-т Октября, 71

✉ Андрей Геннадиевич Стоцкий (stockii_andrei@mail.ru)

Аннотация: Исследована эволюция структуры циркониевого сплава Zr–2,5%Nb при деформации методом равноканального углового прессования (РКУП). Показано, что РКУП при температуре 300 °С приводит к повышению прочностных характери-

стик в 1,4–1,8 раза. Вместе с тем отмечено, что, по сравнению с другими исследованиями, в данном сплаве не происходит полного растворения частиц ниобия, что может быть вызвано замедлением процессов диффузии с понижением температуры деформации до 300 °C. Проведено исследование по предварительной подготовке структуры перед интенсивной пластической деформацией в виде закалки, что позволило сформировать пластинчатую структуру с дополнительными границами. Это способствует измельчению зерна при последующей деформации РКУП. Дополнительно повысить прочность сплава позволяет твердорастворное упрочнение – полное растворение частиц Nb в матрице сплава после закалки. Результатом является повышение в 2,3 раза предела текучести сплава после закалки и РКУП по сравнению с крупнозернистым состоянием.

Ключевые слова: микроструктура, закалка, равноканальное угловое прессование, прочностные характеристики, частицы Nb, циркониевый сплав Zr–2,5%Nb.

Благодарности: Исследование выполнено за счет гранта Российского научного фонда № 20-79-10189-П, <https://rscf.ru/project/23-79-50039/>

Механические испытания и исследования микроструктуры проводились в ЦКП «Нанотех» Уфимского университета науки и технологий.

Для цитирования: Гундеров Д.В., Стоцкий А.Г., Гундерова С.Д., Аубакирова В.Р., Демин А.Ю. Влияние РКУП при температуре 300 °C на структуру и свойства закаленного сплава Zr–2,5%Nb. *Известия вузов. Цветная металлургия*. 2024;30(1):81–92. <https://doi.org/10.17073/0021-3438-2024-1-81-92>

Introduction

Zirconium and its alloys are widely used in such critical applications as nuclear power and medicine. Like titanium, this metal is highly bioinert to the human body [1–4]. Additionally, it is important to note the lower modulus of elasticity of zirconium compared to titanium. This characteristic is crucial for osteoimplants that integrate with human bone, influencing implant acceptance and preventing bone tissue necrosis. Such necrosis may be caused by excessive stress concentration resulting from a significant mismatch between the elastic moduli of the artificial implant and the bone tissue [5; 6]. Stronger materials enable the creation of implants with smaller cross-sections, leading to less traumatic surgery. Therefore, a Zr-based bioinert material that possesses a low modulus of elasticity but higher strength than Zr alloys after conventional treatments is desirable.

Well-known severe plastic deformation (SPD) enhances mechanical properties by grain refining to a nanostructured state [7]. SPD increases strength without altering the chemical composition, thereby preserving biocompatibility, unlike alloying [8; 9]. SPD processes such as equal channel angular pressing (ECAP), multi-axial forging, and rotary swaging enable the production of bulk workpieces/semi-finished products for further processing.

The Zr–2.5%Nb alloy is a renowned zirconium alloy utilized in nuclear power facilities and medical implants. The components of the alloy, zirconium and niobium, are biocompatible. There have been studies [10–13] focused on enhancing the strength of the Zr–2.5%Nb alloy through ECAP.

Typically, the initial coarse-grained structure of the Zr–2.5%Nb alloy consists of a zirconium α -phase and fine niobium particles, present both at the grain boundaries and within the Zr grains. The Zr–2.5%Nb alloy was investigated before and after undergoing ECAP [13]. The initial alloy was obtained through cold rolling followed by annealing at 530 °C for 1 h. It exhibited a two-phase structure: α -phase Zr and some high-temperature β -phase Zr, with Nb dissolved in it. The initial microstructure featured a partially polygonized structure with 100–300 nm grains, a partially recrystallized structure with 1–5 μ m grains, and some β -Nb particles sized 5–15 nm.

The ECAP was carried out in four passes at 430 °C [13]. After ECAP, the Zr–2.5%Nb alloy transitioned to a single-phase structure of niobium solid solution in α -zirconium, with the initial β -phase of zirconium transforming into the α -phase. Studies [10, 13] indicated that, after ECAP deformation at 400 °C, the niobium particles dissolved while the grains refined, leading to a single-phase, ultrafine structure. ECAP effectively refines grains to ultrafine sizes, forming a subgrain/grain structure. After ECAP at 430 °C, equiaxed grains (subgrains) sized between 50 and 200 nm were observed. Initially, the alloy displayed a yield strength of about 380 MPa, a tensile strength of 570 MPa, and a relative elongation at break (δ) of 26 %. Following ECAP ($n = 4$, $t = 430$ °C), yield strength increased by 1.6 times to 620 MPa, and tensile strength to 770 MPa, although δ decreased to 9 %.

Another study [11] performed a more complex ECAP process with temperature reduction between

passes. The Zr–2.5%Nb alloy underwent recrystallization annealing at 580 °C for 6 hours before ECAP, leading to a grain size of 1–2 μm . Subsequently, the metal was processed through isothermal ECAP with a stepwise temperature reduction. Two ECAP modes were applied: 1) two passes at 425 °C followed by two passes at 400 °C and then two passes at 350 °C; 2) two passes each at 450 °C, 425 °C, and 400 °C respectively. The average grain/subgrain size after ECAP Mode 1 was 185 nm. Increasing the final ECAP temperature from 350 to 400 °C (Mode 2) resulted in a predominantly equiaxed structure, with the average grain size growing to 250 nm [11]. XRD analysis revealed α -Zr as the primary phase in the initial alloy with minor amounts of β -Nb and β -Zr. After ECAP Modes 1 and 2, the samples contained only the α -Zr phase, likely due to phase decomposition and particle dissolution in the matrix. The grain refinement and increased dislocation density after ECAP led to a 420 % increase in microstrain. The Zr–2.5%Nb alloy remained a single-phase (α -Zr) material when heated to temperatures between 23 and 490 °C. The second β -Nb phase only formed after annealing at 570 °C [11].

The tensile strength and yield strength of the initial alloy were 420 and 230 MPa, respectively [9], significantly lower than the $\sigma_{\text{ucs}} = 570$ MPa and $\sigma_{\text{ys}} = 380$ MPa of the initial Zr–2.5%Nb alloy as reported in [10; 13]. Mode 1 ECAP with a final temperature of 350 °C, significantly increased tensile strength and yield strength to 820 and 700 MPa, respectively, with $\delta = 10$ % (compared to $\delta = 27$ % for the initial alloy). Mode 2 ECAP, at a final temperature of 400 °C, resulted in tensile strength and yield strength of $\sigma_{\text{ucs}} = 650$ MPa and $\sigma_{\text{ys}} = 470$ MPa, respectively, with $\delta = 14$ % [11]. The analysis of structure thermostability and mechanical properties showed no changes below 350 °C. Annealing the ultrafine-grained Zr–2.5%Nb at 450 °C led to a 15 % decrease in strength due to grain growth, while δ increased to 15–16 %.

Our literature review indicates that ECAP with temperature reduction remains insufficiently explored. Investigating this process for its potential in enhancing strength, refining grains, and achieving structural fragmentation to ultrafine and/or nanoscale levels presents an interesting and significant opportunity. Additionally, it is worth considering quenching as another method to improve microstructure in low-alloy metals by dissolving secondary phases into the base metal.

Additionally, research [14] on high-pressure torsion (HPT) in the Zr–2.5%Nb alloy found a significant in-

crease in microhardness (almost double) compared to the material in its coarse-grained state. This suggests that the Zr–2.5%Nb alloy has the capacity for further grain refinement and enhancement of mechanical properties through ECAP conducted at lower temperatures than those in other studies. Previous research also indicated that quenching the Zr–2.5%Nb zirconium alloy at 890 °C from the β -phase significantly improves its mechanical properties. The aim of this study is to examine the microstructure and mechanical properties of the Zr–2.5%Nb zirconium alloy subjected to ECAP at 300 °C, considering both its coarse-grained state and post-quenching.

1. Materials and methods

We studied the low-alloyed E125 (Zr–2.5%Nb) zirconium alloy. It is a well-known Russian-made biocompatible metal. Its chemical composition is as follows, wt. %: Zr as the base metal; Nb: 2.46; O: 0.032; Fe: 0.001; C: 0.002; and N: 0.0016.

The initial material was the Zr–2.5%Nb alloy after recrystallization annealing at 600 °C for 3 h (herein after referred to as the CG state), and after quenching from the β -phase at 890 °C. We used ECAP tooling with 15 mm diameter channels spaced at 120°. The CG state Zr–2.5%Nb alloy underwent ECAP at 300 °C with 1, 4, and 8 passes. The quenched Zr–2.5%Nb alloy, which initially exhibited higher strength and lower plasticity, was subjected to ECAP at 300 °C with fewer passes: $n = 2$ and 4.

X-ray diffraction (XRD) analysis was performed using an “Ultima IV” diffractometer (Rigaku, Japan) with $\text{CuK}\alpha$ radiation (40 kV, 30 mA).

The metal structure was examined using a JEM 2100 transmission electron microscope (TEM) (Jeol, Japan). The foil samples for transmission electron microscopy (TEM) were 3 mm diameter disks cut from a plate pre-thinned to 100 μm . The disk was electropolished on a “Tenupol-5” machine (Struers, Denmark) using an electrolyte composed of 15 % perchloric acid and 85 % glacial acetic acid. The electropolishing voltage ranged from 22 to 25 V, with a temperature of 15–20 °C. Semi-automatic electropolishing was used until a through-hole appeared.

Flat samples for mechanical tests, measuring $1.1 \times 0.5 \times 4$ mm, were cut from Zr–2.5%Nb billets prepared in various ECAP modes. The mechanical properties were determined by tensile tests at room temperature with a strain rate of $1 \cdot 10^{-3} \text{ s}^{-1}$, performed on an INSTRON 5982 universal testing machine (Instron, USA).

2. Results and discussion

2.1. Microstructure

The Zr–2.5Nb zirconium alloy after recrystallization displays a coarse-grained structure with Zr grain sizes of a few micrometers and some niobium particles. These particles are found both at the Zr grain boundaries and inside the grains, with the average size of the Nb particles being 52 ± 2 nm (Fig. 1, *a*).

After ECAP with 1, 4, and 8 passes, significant changes in the microstructure are observed, as showed in the Fig. 1, *b–d*. A single ECAP pass begins the process of structural refinement and dislocation accumulation, but results in a very heterogeneous structure. The TEM figures reveal areas of refinement (evidenced by small angles between reflexes and identical reciprocal lattices), fragments up to 1 μm with no visible substructure, and individual grains that are weakly deformed (Fig. 1, *b*). The diffraction images of the subgrain structure also show a misorientation of no more than 10° (Fig. 1, *b*). With four passes ($n = 4$), the struc-

ture becomes finer and more homogeneous, including fragmented areas that contain subgrains/grains with an average size of approximately 280 nm (Fig. 2). The presence of niobium particles, indicated with arrows in the figures, and their diffractions showing the reciprocal lattice of niobium are also noted (Fig. 1, *c*). As the number of ECAP passes increases to eight, the microstructure exhibits grains oriented at larger angles and niobium particles. The average size of the grains/subgrains is approximately 260 nm. The evolution of the average grain and subgrain sizes is showed in Fig. 2. The ECAP process also affects the Nb particles, with the smallest particles, a few tens of nanometer in size, dissolving. The particle size decreases only slightly as the number of ECAP passes increases from four to eight (Fig. 2).

The microstructure of the Zr–2.5Nb alloy after quenching exhibits α -Zr oriented lamellae of varying widths, a consequence of the $\beta \rightarrow \alpha$ phase transformation during martensitic quenching, which leads to the formation of α -Zr martensitic lamellae. It is re-

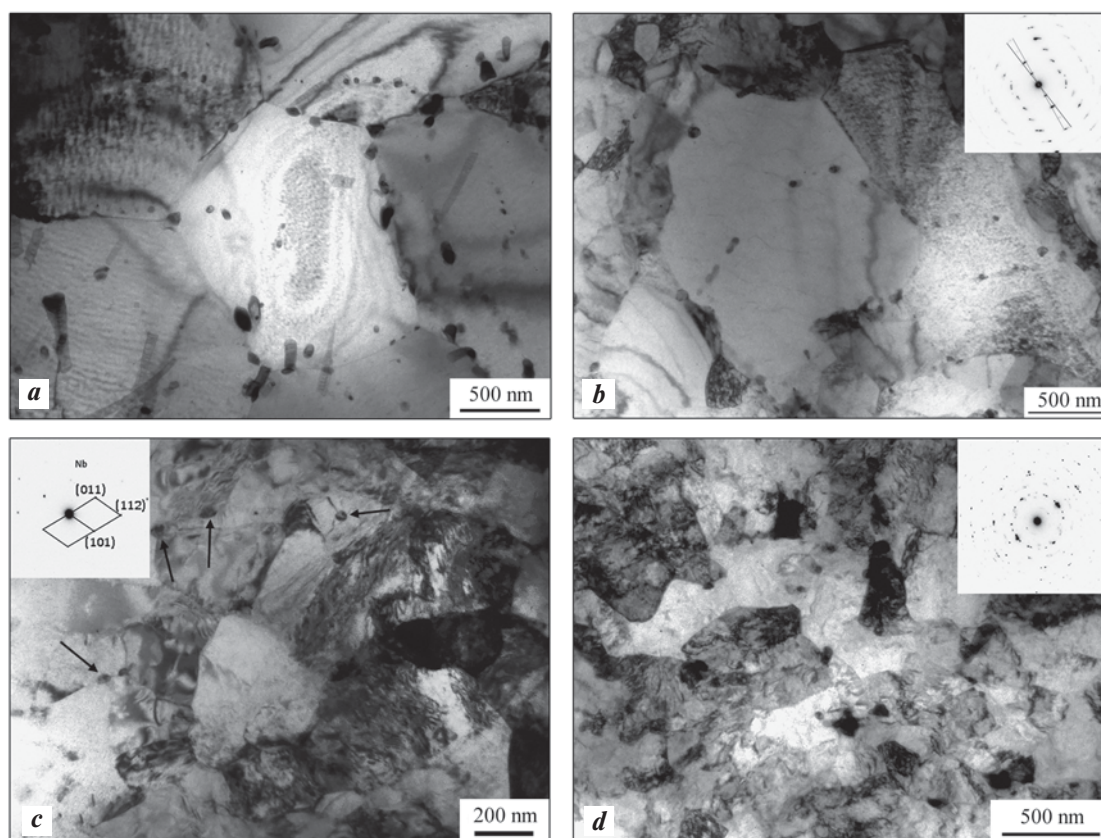


Fig. 1. Microstructure of the Zr–2.5Nb alloy in the CG state (*a*) and after ECAP (*b–d*)

Number of passes: *b* – 1, *c* – 4, *d* – 8

Рис. 1. Микроструктура сплава Zr–2,5Nb в КЗ-состоянии (*a*) и после РКУП (*b–d*)

Число проходов: *b* – 1, *c* – 4, *d* – 8

cognized that at high cooling rates (such as in water), a duplex structure develops in the Zr–2.5Nb alloy, comprising lamellar α -grains formed after the $\beta \rightarrow \alpha$ phase transformation within the original β -grains [15]. After quenching, the Nb particles are completely dissolved, and the niobium atoms forms a solid solution (Fig. 3, *a, b*). Following ECAP with 2 and 4 passes, the lamellae are refined, resulting in the formation of equiaxed grains. With four passes ($n = 4$), lamellae fragmentation becomes more significant compared to two passes ($n = 2$), leading to a structure consisted of ultrafine grains averaging approximately 190 nm in size (Fig. 3, *d*).

XRD analysis reveals that the initial structure of the alloy is predominately the Zr α -phase. While Nikulin S. et al. [11] and Kishore R. et al. [16] suggested the possible presence of the β -Zr phase, the lack of characteristic peaks for the β -phase or their superposition on the Zr α -phase peaks precludes definitive identification of this phase. The XRD analysis also detects a minor amount of the β -Nb phase within the α -Zr matrix, but the (011) peak corresponding to β -Nb is very weak, making it challenging to accurately estimate the volume fraction of this phase from the XRD data (Fig. 4), with its content evidently under 5 %.

XRD results confirm that the primary phase after quenching is α -Zr, as it remains after ECAP in any mode. The potential peaks of the β -Nb and β -Zr phases are either too weak to be discerned or indicate that the alloy is in a single phase. Table 1 details the XRD findings, including a and c , which are the interplanar distances for the (101) peak of the α -phase, Δc representing the dif-

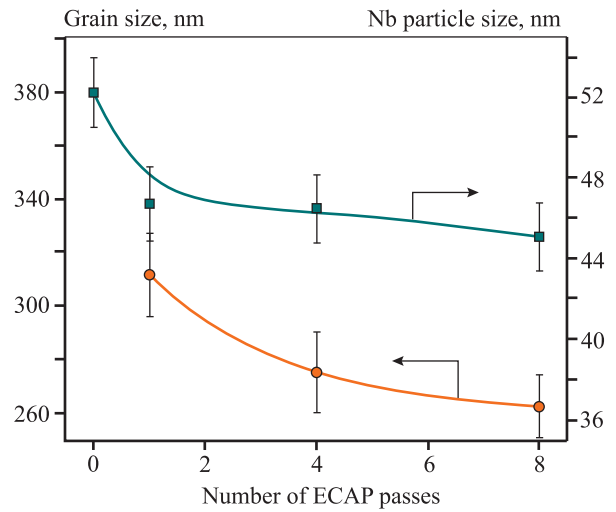


Fig. 2. Variations in the average grain/subgrain and Nb particle size in the Zr–2.5Nb alloy after ECAP

Рис. 2. Изменение среднего размера зерен/субзерен и частиц Nb в сплаве Zr–2,5Nb при деформации методом РКУП

ference in the “ c ” lattice parameters of the α -phase for the initial alloy and the alloy after treatment, coherent scattering regions (CSR), and micro-distortion.

We found that after ECAP with 4 and 8 passes, the lattice parameter c of the Zr–2.5Nb alloy decreases in comparison to the initial alloy. This reduction can be explained by the dissolution of Nb nanoparticles during ECAP, which is also confirmed by TEM. The dissolution of Nb, which has a smaller atomic radius, into the Zr lattice leads to a reduction in the lattice

Tabl. 1. XRD of the Zr–2.5Nb alloy

Таблица 1. Результаты PCA сплава Zr–2,5Nb

State	XRD parameters	a , Å	c , Å	Δc , Å	CSR, nm	Microdistortions ϵ , %
CG (after annealing at 600 °C)		3.2352	5.1605	–	640	0.0007
Quenching ($t = 890$ °C)		3.2231	5.1358	0.0247	780	0.0018
CG + ECAP ($t = 300$ °C, $n = 4$)		3.2318	5.1500	0.0105	527	0.0019
CG + ECAP ($t = 300$ °C, $n = 8$)		3.2302	5.1497	0.0108	475	0.0017
Quenching + ECAP ($t = 300$ °C, $n = 2$)		3.2274	5.1436	0.0168	398	0.0023
Quenching + ECAP ($t = 300$ °C, $n = 4$)		3.2331	5.1526	0.0079	313	0.0026

parameters. After quenching, the “*c*” lattice parameter of the α -phase decreases most significantly due to the complete dissolution of Nb into the Zr lattice. Following quenching and ECAP ($n = 2$, $n = 4$), the para-

meter “*c*” increases relative to the quenched-only state, approaching the value for the initial alloy. This could be due to the decomposition of the solid solution and possible precipitation of Nb nanoparticles, which may

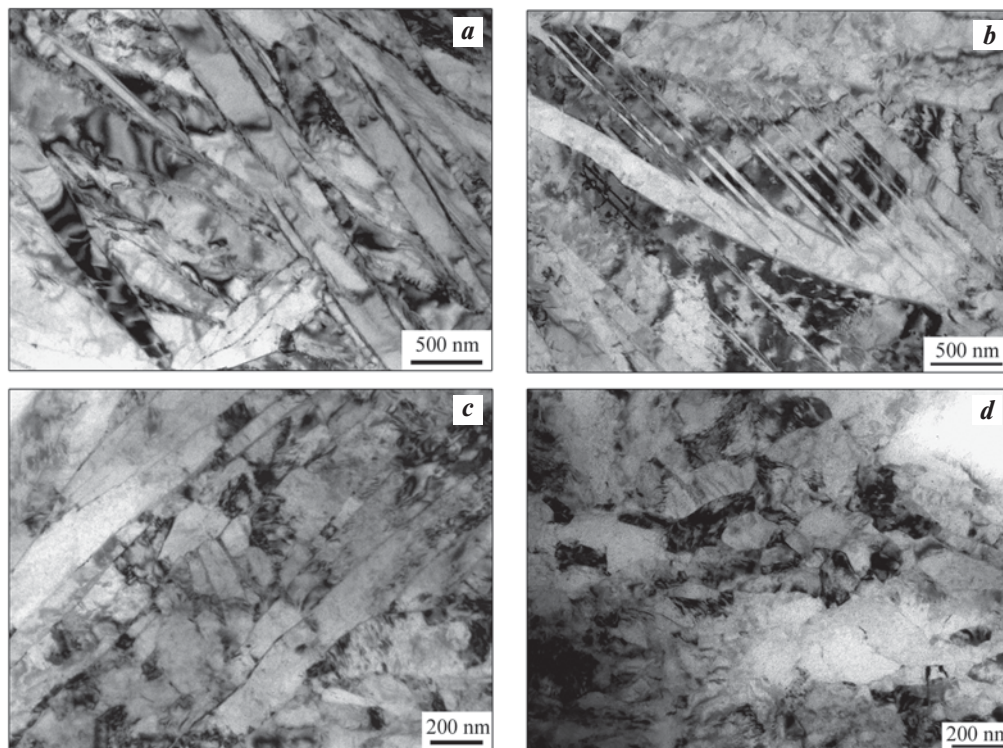


Рис. 3. Микроструктура сплава Zr–2,5Nb после закалки (*a, b*) и после дополнительной РКУП-деформации в 2 прохода (*c*) и 4 прохода (*d*)

Fig. 3. Microstructure of the Zr–2.5Nb alloy after quenching (*a, b*) and following further ECAP in 2 passes (*c*) and 4 passes (*d*)

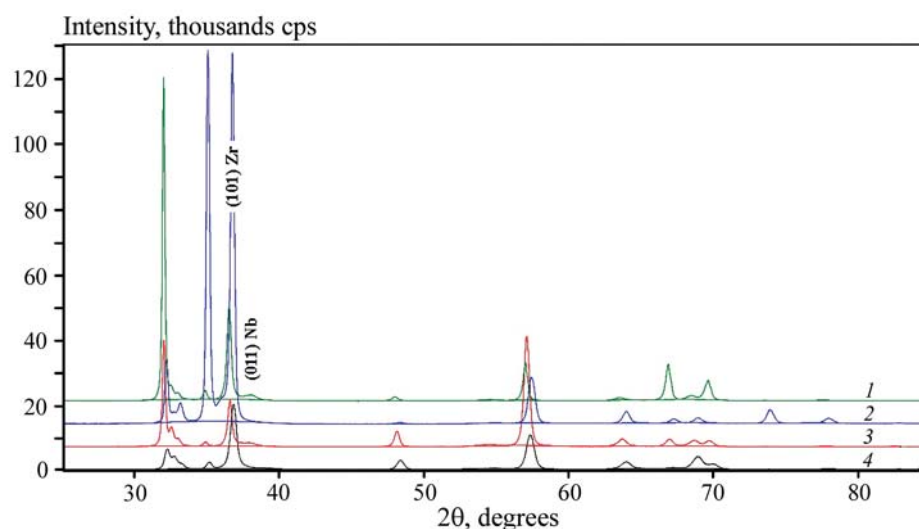


Fig. 4. XRD patterns of the Zr–2.5Nb alloy in various treated states
1 – CG; 2 – quenching; 3 – CG + ECAP ($n = 4$); 4 – quenching + ECAP ($n = 4$)

Рис. 4. Дифрактограммы сплава Zr–2,5Nb в различных состояниях
1 – КЗ; 2 – закалка; 3 – КЗ + РКУП ($n = 4$); 4 – закалка + РКУП ($n = 4$)

be undetectable by TEM because of their small size. As proposed by Straumal B. et al. [17], severe plastic deformation may form a metastable “solid solution—nanoparticles” state with the concentration of the solid solution and the quantity of intermetallic phase dissipation particles being dependent on the equilibrium between the metastable dissolution and phase dissipation processes for the specified SPD, rather than on the initial structure of the alloy [17–19].

With ECAP at $n = 4$ and 8 passes, there is an increase in micro-distortions as a result of grain refinement. However, an increase in the number of ECAP passes from 4 to 8 does not lead to further growth in micro-distortions. Four passes seem sufficient to reach an equilibrium between dislocation formation and relaxation processes under the given SPD conditions [19–21]. Additional passes do not generate extra dislocations; instead, the new dislocations created by further deformation are redistributed to the grain boundaries, causing increased grain misalignment, as indicated by TEM.

After quenching, micro-distortions increase compared to the initial annealed state, likely due to the higher quenching stresses and the formation of a fine lamellar structure. ECAP following quenching leads to further growth in micro-distortions, more so than in the quenched and ECAP-plus-annealing alloys, which is attributed to the grain refinement and higher dislocation density achieved by ECAP. The ECAP of the quenched alloy results in a higher dislocation density and the formation of a more refined structure.

For the commercial alloy, after hot rolling and annealing, the ratio of the XRD peaks corresponding to the Zr α -phase significantly deviates from the nominal value, attributed to the pronounced texturing of the commercial bar. After quenching, the peak ratio for the Zr α -phase shifts, indicating that rapid cooling in water tends to weaken the texture in Zr alloys [22]. It appears that ECAP on the quenched alloy further diminishes and blurs the texture. After quenching + ECAP ($n = 2$) and quenching + ECAP ($n = 4$), the (101) peak of the α -phase emerges as the most intense, aligning with the expected behavior for a texture-free α -phase of Zr.

2.2. Tensile tests

Fig. 5, *a* presents the engineering stress vs. strain curves for the initial alloy and the alloys subjected to ECAP. For comparison, Fig. 5, *b* displays these curves after quenching and subsequent ECAP. Table 2 lists the results of the tensile tests.

Deforming the initial Zr–2.5Nb alloy results in significant hardening. ECAP in 4 and 8 passes increases the strength by 140 to 180 %. After ECAP ($n = 4$, $n = 8$), the ultimate strength rises from 500 to 720 MPa. However, the ductility and uniform elongation decrease from 21.4 to 8.6 % and from 12.0 to 1.3 %, respectively, which is typical for metals after SPD. It is noteworthy that there is no significant increase in strength when the number of ECAP passes increases from 4 to 8. ECAP with $n = 4$ at 300 °C leads to substantial refinement of the structure. Further deformation achieves an equilibrium between refinement and relaxation in the nanostructure [8; 20; 21], hence no further notable refinement of the structure or increase in strength is observed. This is also supported by the micro-distortions detected by XRD. Post-ECAP, the tensile strength and yield strength in the cross section are slightly higher than in the longitudinal direction, a phenomenon also observed in other metals and alloys [9], attributable to the formation of an ECAP-specific texture [9].

Quenching the Zr–2.5Nb alloy significantly increases its strength due to the formation of a lamellar structure, the complete dissolution of Nb particles, and consequently, solid-solution hardening. After quenching at 890 °C, the alloy exhibits improved strength (comparable to that after the initial state + ECAP in 8 passes): 635 MPa yield strength and 718 MPa tensile strength. Plasticity post-quenching drops to 19 %, and the uniform elongation decreases from 12.0 to 3.6 %, typical for hardening through quenching and the formation of a fine lamellar structure. Applying ECAP with $n = 4$ to the quenched alloy increases the yield strength and tensile strength by 120% to $\sigma_{ys} = 772 \pm 11$ MPa and $\sigma_{ucs} = 864 \pm 8$ MPa (longitudinal), with plasticity decreasing from 18.8 to 11.7 %, and uniform elongation to 1.7 %. The strength of 864 ± 8 MPa is slightly higher than that reported [11] after a complex ECAP treatment involving 6 passes with temperature reduction to 350 °C. For ECAP of the quenched alloy, the tensile strength and yield strength in the cross section are slightly higher than in the longitudinal section. So tensile strength and yield strength in the cross section after ECAP of the quenched alloy with $n = 4$ reaching 935 and 846 MPa, respectively. These are the highest values for the current study and for ECAP of the Zr–2.5Nb alloy reported in the literature.

3. Discussion

The structure of the Zr–2.5Nb zirconium alloy in its coarse-grained state consists of equiaxed Zr grains

Tabl. 2. Results of tensile tests for the Zr–2.5Nb alloy

Таблица 2. Результаты механических испытаний сплава Zr–2,5Nb

State	Engineering yield stress σ_{ys} , MPa	Tensile strength σ_{ucs} , MPa	Percent elongation to fracture δ , %	Relative uniform elongation δ_{uni} , %
CG	335 ± 9	500 ± 8	21.4 ± 0.5	12.0 ± 0.8
CG + ECAP ($n = 4$), longitudinal section	601 ± 18	720 ± 6	11.6 ± 1.5	2.1 ± 0.2
CG + ECAP ($n = 4$), cross section	638 ± 14	732 ± 8	8.8 ± 0.3	1.3 ± 0.1
CG + ECAP ($n = 8$), longitudinal section	622 ± 12	724 ± 9	10.4 ± 0.8	1.5 ± 0.5
CG + ECAP ($n = 8$), cross section	658 ± 12	786 ± 5	8.6 ± 0.7	1.4 ± 0.2
Quenching ($t = 890$ °C, $\tau = 30$ min)	635 ± 20	718 ± 10	18.8 ± 0.5	3.6 ± 0.5
Quenching + ECAP ($n = 2$), longitudinal section	750 ± 5	817 ± 16	12.8 ± 0.7	1.5 ± 0.2
Quenching + ECAP ($n = 2$), cross section	784 ± 20	849 ± 11	10.2 ± 0.6	1.1 ± 0.1
Quenching + ECAP ($n = 4$), longitudinal section	772 ± 11	864 ± 8	11.7 ± 0.5	1.7 ± 0.2
Quenching + ECAP ($n = 4$), cross section	846 ± 20	935 ± 15	9.0 ± 0.6	1.2 ± 0.1

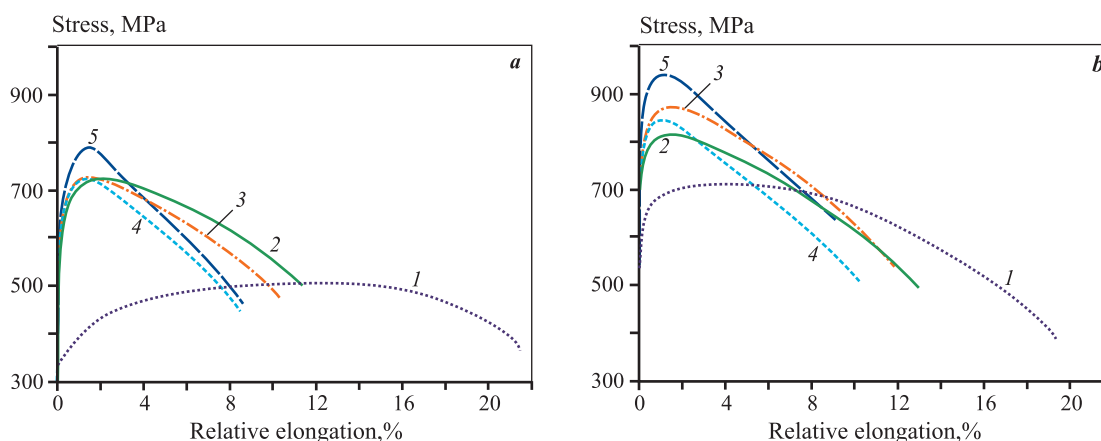


Fig. 5. Mechanical properties of the Zr–2.5Nb alloy in its CG state and after ECAP (a), as well as after quenching + ECAP (b)

a: 1 – CG; 2 – CG + ECAP ($n = 4$), longitudinal section; 3 – CG + ECAP ($n = 8$), longitudinal section;4 – CG + ECAP ($n = 4$), cross section; 5 – CG + ECAP ($n = 8$), cross sectionb: 1 – quenching; 2 – quenching + ECAP ($n = 2$), longitudinal section; 3 – quenching + ECAP ($n = 4$), longitudinal section;4 – quenching + ECAP ($n = 2$), cross section; 5 – quenching + ECAP ($n = 4$), cross section

Рис. 5. Механические свойства сплава Zr–2,5Nb в КЗ-состоянии и после РКУП (a), а также после закалки и РКУП (b)

a: 1 – КЗ; 2 – КЗ + РКУП ($n = 4$), продольное сечение; 3 – КЗ + РКУП ($n = 8$), продольное сечение;4 – КЗ + РКУП ($n = 4$), поперечное сечение; 5 – КЗ + РКУП ($n = 8$), поперечное сечениеb: 1 – закалка; 2 – закалка + РКУП ($n = 2$), продольное сечение; 3 – закалка + РКУП ($n = 4$), продольное сечение;4 – закалка + РКУП ($n = 2$), поперечное сечение; 5 – закалка + РКУП ($n = 4$), поперечное сечение

several micrometers in size and Nb particles, which are often distributed non-uniformly within the grain body and at the grain boundaries. ECAP at 300 °C leads to grain refinement, reducing the grain size to approximately 260 nm. The Nb particles are also refined and partially dissolved due to strain-induced “dissolution” during SPD. Previous studies of ECAP at 400 °C reported complete dissolution of the Nb particles after SPD. It may be attributed to the higher temperature of deformation. ECAP at 300 °C results in incomplete dissolution (as seen in Fig. 1). Potential mechanisms for the dissolution of Nb particles include the active sliding of dislocations through the particles, the formation of vacancies under deformation, and more intense diffusion at an elevated temperature, which all contribute to the transition of Nb atoms into the zirconium lattice, resulting in the partial dissolution of the Nb particles [9].

Reducing the ECAP temperature to 300 °C, compared to 400 °C as studied in [10; 13]), improves structural refinement, and the remaining particles may harden the matrix via the Orowan mechanism. At 300 °C, the yield strength surpasses the values achieved in the above-mentioned studies [10; 13].

Pre-queching of the Zr–2.5Nb alloy dissolves the Nb particles in into the matrix, forms a thin-lamellar structure, and significantly increases strength. Subsequent ECAP of the quenched alloy causes fragmentation of the lamellae and results in the formation of an ultrafine structure with nearly equiaxed grains of ~190 nm in average size. ECAP on the quenched alloy contributes to greater strength growth. Quenching and subsequent ECAP with $n = 4$ results in the highest strength, surpassing that of the initial alloy after ECAP with eight passes.

It is recognized that ECAP deformation for most metals and alloys refines the structure to a grain size of 200 to 300 nm. Typically, to further enhance strength, materials undergo additional ECAP with temperature reduction or other deformation processes, such as drawing, although these approaches can make challenges due to the low ductility of SPD-hardened materials. Nonetheless, specific heat treatments, like quenching or aging, can prepare the initial structure for ECAP by forming additional boundaries that aid grain refinement during ECAP. For the Zr–2.5Nb zirconium alloy, quenching leads to solid-solution hardening due to the dissolution of Nb atoms into the matrix and the creation of numerous martensitic thin-lamellar boundaries in the structure. The greater strength observed after quenching plus four-pass ECAP can be attributed to an increase in solid-solution hardening and a more substantial refine-

ment of the initial thin-lamellar structure. It is also possible that ECAP of the quenched alloy results in a partial decay of the solid solution with potential preprecipitation of the hardening Nb nanoparticles (which may not be detectable by TEM). However, the dissolution of the solid solution is evidenced by the lattice parameter measured by XRD.

Conclusions

The microstructural and mechanical properties analysis of the Zr–2.5%Nb zirconium alloy subjected to ECAP at 300 °C in both its initial coarse-grained state and after quenching revealed several key findings:

1. ECAP led to the refinement of the initial alloy structure, creating boundaries oriented at large angles and forming grains with a size of ~260 nm. However, ECAP at 300 °C did not completely dissolve the Nb particles, which might be attributed to reduced diffusion during strain-induced dissolution, as opposed to what has been noted in other studies at higher temperatures.

2. The strength of the initial alloy increased by 1.4–1.8 times after ECAP with 4 and 8 passes. Conversely, the ductility decreased from 21.4 to 8.6 %, and the uniform elongation decreased from 12.0 to 1.3 %, typical for metals after severe plastic deformation.

3. Pre-treatment via quenching before ECAP developed a thin-lamellar structure, thus creating more boundaries that enhanced grain refinement during ECAP. Quenching also resulted in solid-solution hardening due to the complete dissolution of the Nb particles into the matrix.

4. Mechanical testing indicated that the yield strength of the alloy, once quenched and then subjected to ECAP, was by 2.3 times higher than that of the initial coarse-grained alloy. The ultimate strength in both longitudinal and cross-sectional directions increased to 864 and 935 MPa, respectively. Pre-quenching followed by 4-pass ECAP yielded higher strength than that achieved by 8-pass ECAP without pre-treatment.

References

1. Chopra D., Gulati K., Ivanovski S. Towards clinical translation: optimized fabrication of controlled nanostructures on implant-relevant curved zirconium surfaces. *Nanomaterials*. 2021;11(4):868. <https://doi.org/10.3390/nano11040868>
2. Lee D.B.N., Roberts M., Bluchel C.G., Odell R.A.

- Zirconium: biomedical and nephrological applications. *ASAIO Journal*. 2010;56:550–556.
<https://doi.org/10.1097/MAT.0b013e3181e73f20>
3. Rosalbino F., Macciò D., Giannoni P., Quarto R., Saccone A. Study of the in vitro corrosion behavior and biocompatibility of Zr–2,5Nb and Zr–1.5Nb–1Ta (at.%) crystalline alloys. *Journal of Materials Science: Materials in Medicine*. 2011;22:1293–1302.
<https://doi.org/10.1007/s10856-011-4301-z>
 4. Golovin K.I. Clinico-experimental substantiation of orthopedic treatment with the use of intraosseous zirconium screw implants: Cand. Med. Sci. (PhD in Medicine). Moscow: Moscow State University of Medicine and Dentistry, 2002. (In Russ.).
 Головин К.И. Клинико-экспериментальное обоснование ортопедического лечения с применением внутрикостных винтовых имплантатов из циркония: Автореф. дис. канд. мед. наук. М.: Московский государственный медико-стоматологический университет, 2002.
 5. AlFarraj A.A., Sukumaran A., Al Amri M.D., Van Oirschot A.B., Jansen J.A. A comparative study of the bone contact to zirconium and titanium implants after 8 weeks of implantation in rabbit femoral condyles. *Odontology*. 2018;106:37–44.
<https://doi.org/10.1007/s10266-017-0296-3>
 6. He X., Reichl F.-X., Milz S., Michalke B., Wu X., Sprecher C.M., Yang Y., Gahlert M., Röhling S., Kniha H., Hickel R., Högg C. Titanium and zirconium release from titanium- and zirconia implants in mini pig maxillae and their toxicity in vitro. *Dental Materials*. 2020;36:402–412.
<https://doi.org/10.1016/j.dental.2020.01.013>
 7. Valiev R.Z., Zhilyaev A.P., Langdon T.G. Bulk nanostructured materials: fundamentals and applications. 1st ed. Wiley, 2013.
 8. Zhilyaev A.P., Valiev R.Z., Langdon T.G. Ultrafine-grained metallic materials and coatings. *Advanced Engineering Materials*. 2020;22(10):2001012.
<https://doi.org/10.1002/adem.202001012>
 9. Valiev R.Z., Parfenov E.V., Raab G.I., Semenova I.P., Dluhoš L. Bulk nanostructured metals for advanced medical implants and devices. In: *IOP Conference Series: Materials Science and Engineering. 5th International Conference Recent Trends in Structural Materials* (14–16 November 2018). 2018;461:012089.
<https://doi.org/10.1088/1757-899X/461/1/012089>
 10. Terent'ev V.F., Dobatkin S.V., Nikulin S.A., Kopylov V.I., Prosvirin D.V., Rogachev S.O., Bannykh I.O. Effect of equal-channel angular pressing on the fatigue strength of titanium and a zirconium alloy. *Russian Metallurgy (Metally)*. 2011;201:981–988.
<https://doi.org/10.1134/S003602951100119>
 11. Nikulin S.A., Rozhnov A.B., Rogachev S.O., Khatkevich V.M., Turchenko V.A., Khotulev E.S. Investigation of structure, phase composition, and mechanical properties of Zr–2,5% Nb alloy after ECAP. *Materials Letters*. 2016;169:223–226.
<https://doi.org/10.1016/j.matlet.2016.01.148>
 12. Nikulin S.A., Rogachev S.O., Rozhnov A.B., Gorshenkov M.V., Kopylov V.I., Dobatkin S.V. Resistance of alloy Zr–2,5%Nb with ultrafine-grain structure to stress corrosion cracking. *Metal Science and Heat Treatment*. 2012;54:407–413.
<https://doi.org/10.1007/s11041-012-9522-3>
 13. Kukareko V.A., Kopylov V.I., Kononov A.G., Rogachev S.O., Nikulin S.A., Dobatkin S.V. Structural transformations during heating of a Zr–2,5%Nb alloy subjected to equal-channel angular pressing. *Russian Metallurgy (Metally)*. 2010;2010:642–647.
<https://doi.org/10.1134/S0036029510070116>
 14. Gunderov D., Stotskiy A., Lebedev Y., Mukaeva V. Influence of HPT and accumulative high-pressure torsion on the structure and Hv of a zirconium alloy. *Metals*. 2021;11(4):573.
<https://doi.org/10.3390/met11040573>
 15. Chai L., Xia J., Zhi Y., Chen K., Wang T., Song B., Guo N. Strengthening or weakening texture intensity of Zr alloy by modifying cooling rates from $\alpha + \beta$ region. *Materials Chemistry Physics*. 2018;213:414–421.
 16. Kishore R., Singh R.N., Dey G.K., Sinha T.K. Age hardening of cold-worked Zr–2,5wt%Nb pressure tube alloy. *Journal of Nuclear Materials*. 1992;187:70–73.
[https://doi.org/10.1016/0022-3115\(92\)90320-K](https://doi.org/10.1016/0022-3115(92)90320-K)
 17. Straumal B.B., Zavorotnev Yu.D., Davdyan G.S. High-pressure torsion and phase transformations in metal alloys. *Physics and High Pressure Technology*. 2022;32(4):5–29. (In Russ.).
 Страумал Б.Б., Заворотнев Ю.Д., Давдян Г.С. Кручение под высоким давлением и фазовые превращения в металлических сплавах. *Физика и техника высоких давлений*. 2022;32(4):5–29.
 18. Glaser A.M., Sundeev R.V., Shalimova A.V., Metlov L.S. Physics of severe plastic deformation. *Physics—Uspekhi*. 2023;66(1):32–58.
<https://doi.org/10.3367/UFNr.2021.07.039024>

- Глезер А.М., Сундеев Р.В., Шалимова А.В., Метлов Л.С. Физика больших пластических деформаций. *Успехи физических наук*. 2023;193(1):33–62. <https://doi.org/10.3367/UFNr.2021.07.039024>
19. Gunderov D.V. Some regularities of amorphization and nanocrystallization at intensive plastic deformation of crystalline and amorphous multicomponent alloys. *Investigated in Russia (Electronic journal)*. 2006;151:1404–1413. (In Russ.).
Гундеров Д.В. Некоторые закономерности аморфизации и нанокристаллизации при интенсивной пластической деформации кристаллических и аморфных многокомпонентных сплавов. *Исследовано в России (электронный журнал)*. 2006;151:1404–1413.
20. Razumov I.K., Yermakov A.E., Gornostyrev Y.N., Straumal B.B. Nonequilibrium phase transformations in alloys under severe plastic deformation. *Physics—Uspekhi*. 2020;63:733–757. <https://doi.org/10.3367/UFNe.2019.10.038671>
- Разумов И.К., Ермаков А.Е., Горностырев Ю.Н., Страумал Б.Б. Неравновесные фазовые превращения в сплавах при интенсивной пластической деформации. *Успехи физических наук*. 2020;190:785–810. <https://doi.org/10.3367/UFNe.2019.10.038671>
21. Teitel I., Metlov L.S., Gunderov D.V., Korznikov A.V. On the nature of structural and phase transformations induced by severe plastic deformations in solids. *Physics of Metals and Metallurgy*. 2012;113(12):1–8. (In Russ.).
Тейтель И., Метлов Л.С., Гундеров Д.В., Корзников А.В. О природе индуцируемых интенсивными пластическими деформациями структурных и фазовых превращениях в твердых телах. *Физика металлов и металловедение*. 2012;113(12):1–8.
22. Chai L., Xia J., Zhi Y., Chen K., Wang T., Song B., Guo N. Strengthening or weakening texture intensity of Zr alloy by modifying cooling rates from $\alpha + \beta$ region. *Materials Chemistry and Physics*. 2018;213:414–421. <https://doi.org/10.1016/j.matchemphys.2018.04.044>

Information about the authors

Dmitry V. Gunderov – Dr. Sci. (Phys.-Math.), Head Researcher of the Institute of Physics of Molecules and Crystals, Chief Researcher of the Ufa University of Science and Technology.

<https://orcid.org/0000-0001-5925-4513>

E-mail: dimagun@mail.ru

Andrey G. Stotskiy – Junior Researcher, Ufa University of Science and Technology.

<https://orcid.org/0000-0002-2667-1115>

E-mail: stockii_andrei@mail.ru

Sofia D. Gunderova – Undergraduate Student of the Ufa University of Science and Technology, Research Laboratory Assistant of the Institute of Physics of Molecules and Crystals.

<https://orcid.org/0009-0005-7986-8156>

E-mail: gynderova@mail.ru

Veta R. Aubakirova – Cand. Sci. (Eng.), Senior Researcher, Ufa University of Science and Technology.

<https://orcid.org/0000-0002-8483-6408>

E-mail: veta_mr@mail.ru

Alexey Yu. Demin – Dr. Sci. (Eng.), Associate Prof., Head of the Department of Electronic Engineering, Ufa University of Science and Technology.

<https://orcid.org/0000-0002-6668-3356>

E-mail: deminal77@yandex.ru

Информация об авторах

Дмитрий Валерьевич Гундеров – д.ф.-м.н., вед. науч. сотрудник Института физики молекул и кристаллов (ИФМК) УФИЦ РАН, гл. науч. сотрудник Уфимского университета науки и технологий (УУНиТ).

<https://orcid.org/0000-0001-5925-4513>

E-mail: dimagun@mail.ru

Андрей Геннадиевич Стоцкий – мл. науч. сотрудник УУНиТ.

<https://orcid.org/0000-0002-2667-1115>

E-mail: stockii_andrei@mail.ru

Софья Дмитриевна Гундерова – студент бакалавриата УУНиТ, лаборант-исследователь ИФМК УФИЦ РАН.

<https://orcid.org/0009-0005-7986-8156>

E-mail: gynderova@mail.ru

Вета Робертовна Аубакирова – к.т.н., ст. науч. сотрудник УУНиТ.

<https://orcid.org/0000-0002-8483-6408>

E-mail: veta_mr@mail.ru

Алексей Юрьевич Демин – д.т.н., доцент, заведующий кафедрой электронной инженерии УУНиТ.

<https://orcid.org/0000-0002-6668-3356>

E-mail: deminal77@yandex.ru

Contribution of the authors

D.V. Gunderov – defined the problem statement and study concept, authored the paper.

A.G. Stotskiy – conducted studies on microstructure and mechanical properties, contributed to paper authoring and discussions.

S.D. Gunderova – performed XRD analysis, participated in discussions.

V.R. Aubakirova – contributed to paper authoring and discussions.

A.Yu. Demin – authored the paper, analyzed the results.

Вклад авторов

Д.В. Гундеров – определение цели работы и ее концепции, участие в написании статьи.

А.Г. Стоцкий – исследование микроструктуры и механических свойств, участие в написании статьи и в обсуждении результатов.

С.Д. Гундерова – проведение рентгенофазового анализа, участие в обсуждении результатов.

В.Р. Аубакирова – участие в написании статьи и обсуждении результатов.

А.Ю. Демин – участие в написании статьи, анализ результатов.

The article was submitted 11.12.2023, revised 26.01.2024, accepted for publication 07.02.2024

Статья поступила в редакцию 11.12.2023, доработана 26.01.2024, подписана в печать 07.02.2024